Ulysses Out-of-ecliptic Observations of Interplanetary Shocks

M.E. Burton, E.J. Smith,
Jet Propulsion Laboratory, Pasadena CA
A. Balogh, R.J. Forsyth,
imperial College of Science and Technology, Blackett Laboratory, London U.K.
S.J. Bame, Phillips, Los Alamos National Laboratory, Los Alamos, N.M.
B.E. Goldstein
Jet Propulsion Laboratory, Pasadena, CA

Abstract

interplanetary shocks observed at the Ulysses spacecraft as it traveled from the ecliptic plane to the southern solar pole have been identified and analyzed using both magnetic field and plasma measurements. The latitude dependence of various parameters associated with the shocks (beta, θ_{BN} and Mach number) have been investigated. The direction of shock propagation of forward and reverse corotating shocks is qualitatively consistent with the global 3-D model of Pizzo [1991] which predicts that forward shocks will propagate equatorward while reverse shocks propagate poleward. The strongest shocks, are observed at mid-latitudes and are from the south polar coronal hole. These shocks are shown to be supercritical in contrast to the lower latitude sub-critical shocks. This change in character of the shocks is likely related to the intensity of the shock-accelerated energetic particles which also peaks in the same latitude range.

Introduction

Properties of interplanetary shocks in or near the ecliptic plane have previously been examined using data from various spacecraft over many years. Both corotating and transient shocks have been observed throughout the solar cycle at a wide range of distances from Helios in the inner heliosphere [Volkmer and Neubauer, 1985] to Pioneer and Voyager in the outer heliosphere [see Smith, 1985 for a summary of these observations]. Ulysses, in transit to Jupiter has also contributed to the wealth of shock observations in the ecliptic plane [Burton et al., 1992, Balogh et al., 1995].

The out-of-ecliptic portion of the Ulysses mission provided the first opportunity to search for and study interplanetary shocks at high latitudes. Ulysses flew by Jupiter (-5 AU) in February, 1992, employing a gravity assist to achieve an out-of-ecliptic trajectory and by September, 1994 had reached its maximum latitude of 80.2 degrees. Using high resolution magnetic field and plasma data, interplanetary shocks from Jupiter encounter through mid-September, 1994 have been identified and analyzed. We present the out-of-ecliptic shock observations, examine the latitude dependence of shock properties and discuss the implications.

Analysis: Identification, Determination of shock normals and speeds

preliminary identification of interplanetary shocks was carried out using both magnetic field and plasma data. Details of the instruments can be found in Balogh et al. [1992] and Bame et al. [1992]. 'I"he criterion used to classify an event as a shock is a sonic Mach number, $M=V_s/C_f$ greater than one. C_f, the fast mode speed, is calculated using the ion sound speed, the Alfven speed and θ_{BN} (the angle between the shock

normal and the upstream field) and thus relies on both the magnetic field and plasma data. V_s is the shock velocity in the upstream solar wind frame.

θ_{BN} was accurately determined by transforming the data into shock coordinates. This method relies on magnetic coplanarity [Colburn and Sonett, 1966] which requires that the field on both sides of the shock (and therefore AB) lie in a plane containing the shock normal. Over the last several years, we have used a computer algorithm that transforms high time resolution magnetic field data directly into shock coordinates with one axis along ΔB and another axis (x) lying along the shock normal. The advantages of the method are simplicity, the high time resolution provided by the rapid field measurements, the elimination of the necessity to define the time intervals upstream and downstream of the shock and the determination of the shock coordinates in a least squares sense. It results in a data plot in shock coordinates which can be inspected immediately to see how satisfactory the fit is and to assess the possible presence of time variations associated, for example, with nearby hydromagnetic discontinuities.

The first step is to carry out a variance analysis [Sonnerup and Cahill, 1967] of' $\vec{B}$ over an (arbitrary) interval approximately centered on the shock. The direction corresponding to the largest eigenvalue is identified with the field jump and defines the z-axis. The field vectors are then transformed into an intermediate coordinate system having one axis along this direction, one of the axes in the original system being used to define the prime meridian. The averages of the two field components transverse to z yield the angle through which to rotate so that one of the component averages is zero. This operation defines the y-axis and the orthogonal (x) axis is the direction of the normal. If desired, the time interval can be changed and the analysis repeated. The θ_{BN} values obtained using this technique have been compared with those determined

using the mixed-mode method [A braham-Shrauner and Yun, 1976] which relies on coplanarity of the upstream and downstream velocity vectors. For 75% of the shocks the two methods agreed within 10°, lending confidence to our determination of the normals.

The shock velocity $V_S = |\Delta\vec{V} \times \vec{B}_2| / \vec{B}_2 - \vec{B}_1$ was calculated from the formulation of Smith and Burton [1988]. The relation is interpretable as conservation of the electric field in the frame of reference of the shock and has advantages over the expression based on conservation of mass since the magnetic field is measured more accurately and sampled more rapidly than the plasma density.

Using θ_{BN}, the shock velocity, and the fast mode speed the Mach number was calculated. Many events with Mach numbers less than one were found. Although they may represent waves that have not yet steepened into shocks, they are not included in this study. During the nearly two and a half years of out-of-ecliptic observations, 80 shocks were identified, 42 forward shocks and 38 reverse shocks. Most of these events are tabulated in Balogh et al. [1995].

Figure 1 provides a complete summary of shock observations through the end of 1993. Forward (up-arrow) and reverse (down-arrow) shocks are shown superposed on hour averages of the magnetic field magnitude and solar wind velocity. Heliographic latitude and radial distance are shown at the top of the field panels.

As is evident, Ulysses sampled widely varying solar wind conditions [Gonzalez-Esparza et al., 1996]. From February until July 1992 (-day 180), the solar wind consisted of small irregular corotating streams as well as transients driven by coronal mass ejections (region A in figure 1). In July, 1992, a stream emanating from a polar coronal hole was observed and continued to dominate the solar wind structure

through mid-1993 (region B). By day 120, May, 1993, at a latitude of 30° S and a distance of 4.7 AU, the heliospheric current sheet (HCS) ceased to be seen at Ulysses [Smith et al., 1993]. A region of intermediate velocity solar wind continued to be observed for four more solar rotations (region C). In late July, 1993 through its maximum latitude, Ulysses was immersed in high speed solar wind, with speeds consistently in the 700 to 800 km s^{-1} range (region D) [Phillips et al, 1994]. The disappearance of structure in the magnetic field was coincident with the solar wind velocity remaining at a high approximately constant value.

Latitude Dependence of Shock Properties

Figure 2 shows the number of shocks observed per day per 5° heliographic latitude interval. The number of forward and reverse shocks as well as the total number of shocks are shown. Near the ecliptic plane, reverse shocks occur at roughly one per solar rotation (0.04/day). Twice as many forward shocks are seen. As the streams develop and the spacecraft climbs in latitude, the frequency of occurrence of forward shocks declines with forward and reverse shocks occurring in equal numbers by 25° latitude. Coincident with the disappearance of the heliospheric current sheet and the surrounding slow solar wind at 30° latitude, there is an almost total disappearance of forward shocks accompanied by an enhancement in reverse shock occurrence. At higher latitudes the number of reverse shocks decreases. By 45° latitude, reverse shocks are seen at a frequency of one every two solar rotations and forward shocks are rarely seen. No forward shock was seen at latitudes greater than 54° S except for a few that were clearly associated with CMEs. The highest latitude reverse shock was

observed at 610 S. Many of these observations have been previously reported [Gosling et al., 1993].

A subset of shocks from which the most obvious transient-related events have been eliminated was used to investigate the latitude dependence of corotating shock properties. The three variables, θ_{BN} beta and Mach number, customarily used to characterize an interplanetary shock are shown in figure 3 as a function of latitude. Circles indicate parameters associated with forward shocks and triangles identify those associated with reverse shocks. The data are binned in five degree latitude increments except for the two highest intervals. Because the frequency of both forward and reverse shocks decreases with latitude, the bin size was changed to accumulate a sufficient number of events to calculate statistically meaningful averages. 'l'he averages are plotted in the centers of the bins.

There is a tendency for θ_{BN} (figure 3a) to increase as Ulysses leaves the ecliptic plane. By 20° latitude both forward and reverse shocks tend to be quasi-perpendicular. With increasing latitude, the decrease in θ_{BN} probably reflects an increasingly radial magnetic field. However, at high latitude, θ_{BN} for the reverse shocks is still 50°-600. Beta (panel b) upstream of the shocks varies systematically with latitude. It is relatively constant near the ecliptic plane but increases dramatically above 25° latitude. After the disappearance of the current sheet above 30°, beta decreases to values nearer those in the ecliptic plane, Panel c shows that the Mach numbers are highest for both forward and reverse shocks when associated with the large corotating streams and tend to decline with increasing latitude. Reverse shocks at latitudes above the current sheet are weak with an average Mach number of on] y 1.7.

Parameters related to shock strength (binned in a similar manner to figure 3) are shown in figure 4. Panel a shows the ratios of the field strengths downstream and upstream of the shock. The values are largest in region B. Panel b shows the shock velocity. A strong peak occurs for reverse shocks in region B. An additional parameter which has proven useful in characterizing shocks is the first critical Mach number as defined by Kennel [1 987]. This Mach number has been determined for our subset of corotating shocks and the ratio of shock Mach number to critical Mach number is shown in figure 4c. Shocks that have a value greater than one are supercritical. The majority of shocks are subcritical with the notable exception of those associated with the large corotating streams (region B). At higher latitudes, both forward and reverse shocks are subcritical.

Shock Normal Orientation

The direction of propagation of the corotating shock fronts has been investigated using the shock normal orientation. According to the global model of Pizzo [1991] corotating shock fronts should be organized by the inclination of the solar magnetic dipole or, equivalently, the HCS. To test this model, we have projected the shock normals onto the dipole axis whose orientation was obtained from the source surface contours [Solar Geophysical Data, 1992-3].

In the simplest model, the heliospheric current sheet to the magnetic dipole axis ($\vec{m}$). In this case, the neutral line is a perfect sinusoid. The longitude of the dipole coincides with the maximum latitudinal excursion of the neutral line in the southern hemisphere. The maximum extent of the neutral line in latitude defines the tilt angle between the dipole and the solar rotation axis. Although the neutral line topology can

rarely be represented by a simple sinusoid, this scheme can be used to obtain an estimate of the dipole orientation.

Given the latitude and longitude, the orientation of the magnetic dipole, ($\vec{m}$) is calculated in the Solar-Interplanetary coordinate system in which the magnetic field data are analyzed. The frequency distributions of the angle between $\vec{n}$ and m are shown separately for forward (figure 5a) and reverse shocks (figure 5b). In the southern hemisphere a value of zero degrees indicates equatorward propagation aligned with the dipole axis while 180 degrees implies poleward propagation. Forty percent of the forward shock normals lie within 30° of the dipole axis and thirty percent of the reverse shock normals lie within 30° of the opposite direction. The asymmetric behavior of the forward and reverse shocks is evident.

These distributions have been normalized to account for the "solid angle effect". Since the magnetic dipole axis represents the pole of a hemisphere, the probability of observing a shock normal at a given angle is a function of the solid angle enclosed. For an isotropic distribution, the probability of observing a normal nearly parallel to the dipole axis is much less than that of observing a normal aligned nearly perpendicular to the axis. Simple geometrical considerations show that the probability of the normal occupying a range of angles between α_1 and α_2 is proportional to cos (α_1) - cos (α_2) = A cos (α). The distributions have therefore been normalized by dividing the number of observed cases in each bin by the reciprocal of A cos (α) to correct for this effect,

A graphical representation of these results is obtained by projecting the shock normals onto the r,δ plane formed by the vectors in the radial and latitudinal directions, as in figures 6a and 6b. The forward shocks propagate both equatorward and poleward at low latitudes but the tendency for the highest latitude shocks to propagate

equatorward can be seen, The reverse shocks also propagate in both directions near the solar equator but poleward at higher latitudes. (> 40° S).

The presence of shocks traveling both equatorward and poleward at low latitudes is consistent with the Pizzo [1991] model. At latitudes dominated by the current sheet (or heliomagnetic streamer belt), the directions of propagation are determined by the local tilt which alternates between clockwise and counter-clockwise angles. It is only when the spacecraft is above this low latitude region that purely equatorward or poleward propagation is expected for forward and reverse shocks, respectively.

Discussion

Shock Occurrence as a function of Latitude

Interplanetary shocks observed at Ulysses from the ecliptic plane to its maximum latitude of 80.2° over the Sun's southern pole have been identified and analyzed. The rate of occurrence of interplanetary shocks has decreased dramatically with latitude, The few shocks observed at high latitude can be characterized as low Mach number, low beta, reverse shocks.

Various possibilities can be invoked to explain the decrease in shock occurrence. A qualitative geometrical argument first suggested by Siscoe [1976] predicted that fewer shocks would be observed at high latitudes. The pitches of fast. and slow solar wind streamlines converge since the fast streamline is more radial. At higher latitudes, the pitches of the streamlines are less than at the equator and they converge, and the shock forms, at greater distance. Using a mathematical formulation of the argument an estimate of the heliocentric distance to the inner edge of a corotating

shock wave, R, as a function of latitude was obtained. R increased away from the equator but always remained between the distance at which the shock forms in the equator, R_{eq}, and $R_{eq}/\sin\theta$, where 0 is the colatitude.

A separate effect influencing shock formation is the relative velocity of the streams [Siscoe, 1976]. The greater the relative velocity, the closer to the sun the shock wave forms, the effect again being due to the relative pitch of the fast and slow streamlines. The dramatic decrease in frequency of occurrence at high latitude can be explained in part by the decrease in relative velocity evident in figure 1.

The global model of Pizzo [1982,1991 ,1994] suggests an additional explanation for the decreased frequency of occurrence. This model considers interaction regions tilted with respect to the equatorial plane. The model is applicable during the interval of our study, the late declining and minimum phase of the solar cycle, when the large-scale coronal magnetic field has a tilted dipole configuration. Systematic meridional flow deflections have been reported in the Ulysses plasma data that are consistent with forward waves propagating antisunward, westward and equatorward and reverse waves propagating sunward, eastward and poleward [Gosling et al., 1993, Gosling et al., 1995]. A further test of the model is provided by our analysis of the shock propagation direction as determined from the shock normal orientation. The forward and reverse shocks tend to be parallel to the tilted interaction regions with the normals to the forward shock slanted equatorward and the reverse shock normal slanted poleward. The observed directions are qualitatively consistent with this model.

The basic feature of the model is a band of slow solar wind at low latitude and fast solar wind emanating from the polar region. While these conditions are generally

observed at Ulysses the actual configuration of the solar magnetic field is somewhat more complicated. Positive polarity equatorial coronal holes are consistently observed in the 1083 nm coronal hole maps produced by the Kitt Peak Observatory during this interval and account for the positive polarities observed at Ulysses. Figure 7 shows the configuration of the solar corona and the corresponding source surface contour representative of this interval. This configuration implies that high speed solar wind originates at low latitudes also. A 3-D simulation appropriate to equatorial coronal holes would be a useful extension of the Pizzo-type model.

Shock Structure as a Function of Latitude

The Ulysses observations reveal a significant change in the character of CIR shocks with latitude. In the interval when the sequence of high speed streams is occurring (region B) and the spacecraft is at latitudes between -15° and -30°, the shocks are found to be supercritical in contrast to the shocks observed at lower latitudes. Basically, supercritical shocks occur when the Mach number becomes large enough that the solar wind ions as well as the electrons contribute to the dissipation and structure, e.g., an overshoot in the magnetic field profile. Other related changes with latitude occur in θ_{BN} and B. The observations raise two questions: What causes these changes? To what extent do they represent a latitude dependence rather than a temporal variation?

Of the three basic parameters characterizing shocks, only beta is dependent on upstream parameters (n, T,B) and independent of shock geometry. The shock normal angle θ_{BN}, depends on $\vec{n}$ as well as on the upstream field direction. The Mach number depends on the shock speed which is related to the velocity jump across the shock and

is a measure of the shock strength. The fast mode phase speed depends principally on the upstream parameters represented by the ion sound speed, C_s, and the Alfven speed, C_A, as well as on θ_{BN}.

The increase in plasma beta with latitude in region B is explainable in terms of an increase in plasma temperature, Since n tends to be proportional to r-2 and B to r^{-1} n/B^2 in the unperturbed solar wind upstream of both the forward shock anti reverse shock should be approximately constant. Hence, beta is proportional to T. The well-known correlation between T and V implies that beta will increase, upstream of the shocks, a feature observable in figure 3b. Figure 8 shows both the ion density and the ion beta computed over 5 degree latitude intervals. The slight decrease in 'density is unrelated to the increase in beta in agreement with our expectations.

Figure 3a shows a decrease of θ_{BN} in region B that is seen in both the forward and reverse shocks. Such a change might not be anticipated if the Parker spiral angle is over-emphasized. In a reference frame corotating with the Sun, the solar wind streamlines are parallel to the spiraled magnetic field and, at large radial distances, the field on average is expected to be tightly wound. Thus, the shock geometry inferred from converging streamlines would be quasi-perpendicular with $\theta_{BN} \cong 90°$, However, the average θ_{BN} is $\cong 50°$ at all latitudes.

A likely explanation is that the lower average value of θ_{BN} is the consequence of the ever-present fluctuations in field direction. Basically, the fluctuations will cause the average upstream angle to be less than 90°. This conclusion follows from considering the probability distribution of the spiral angle combined with the fact that θ_{BN} is restricted to the positive range from 0°- 90°. Ulysses studies have shown that the variances in field direction increase significant y with latitude [Smith et al., 1995].

This hypothesis has been tested by simulating θ_{BN}, the results being shown in figure 9. We identify the corotating shock normals with the perpendicular to the Parker spiral angle, Ψ_P. This condition is equivalent to assuming $\vec{n}$ II (90 - Ψ p) or perpendicular shocks. The actual spiral angle, Ψ_B, was determined upstream of the observed forward and reverse shocks and was subtracted from 90- Ψ_P to obtain the synthetic θ_{BN}. The results are shown in the upper panel and compare very favorably with the observed values which are repeated in the lower panel. We, therefore attribute the decrease in average θ_{BN} at higher latitudes to the effect of the increasing variability in field direction.

The related increases in M_f, V_s and AV at higher latitude are explainable as a consequence of the large velocity gradient associated with the large amplitude high speed streams. The speed increases from $\cong$ 400 to $\cong$ 800 km/see should result in greater compression of the plasma interface region and lead to higher pressures. The resulting stresses directed outward from the stream interface will generate faster large amplitude waves which will then steepen into shocks. To test this hypothesis, we computed the peak pressures at the interfaces between the slow and fast wind. The interfaces are identified by the peaks in |B| and the total internal plasma pressure, $p = nk(T_i + T_e) + B^2/8\pi$. The pressures at the interfaces are shown in figure 10. They increase markedly in region B as predicted.

The realization that the supercritical shocks depend on the character of the high speed streams in region B is relevant to the question of whether or not supercritical shocks would have been observed at higher latitudes in the absence of the high speed streams seen in the ecliptic at the same time. The appearance of the streams just as Ulysses descended from 15° to 30° is a temporal effect. Such streams are known to be

a feature of the declining phase in solar activity having been observed in 1973, 1984 and now 1994. Furthermore, the high speed streams were simultaneously observed in the ecliptic by IMP-8 and in the outer heliosphere by Voyager 2.

However, the highest speed streams observed at Ulysses may exceed those seen in the ecliptic because of the latitude difference, i.e., higher speeds toward the center of the south polar coronal hole. This effect is likely to be of secondary importance to the stream structure generally but could be important to the development of the supercritical shocks, To do more than speculate about such effects is outside the scope of the present study.

It may be that observations over the same range of latitudes at a different phase of the solar cycle will not reproduce those reported here. Since the corotating shocks only form well beyond 1 AU, observations in the ecliptic near Earth's orbit are marginally useful in testing this presumption. However, Ulysses will again cover the same latitude range at comparable heliocentric distances during its descent from the Sun's north polar cap in 1996-7. Continued observations by Ulysses should provide another opportunity to revisit the questions raised here.

Shock structure and energetic particles

Although the Ulysses observations of supercritical shocks may be solar cycle dependent, they provide a unique opportunity to study the effect of shock structure on the local acceleration of energetic particles by shock drift acceleration and/or diffusive shock acceleration. A thorough comparison of the changing shock properties with the properties of energetic particles is needed. However, for now, we simply point out the obvious correspondence between the broad maximum in energetic particle intensity

between 10° and 30° latitude reported by Sanderson et al. [1994] and the appearance of the stronger, supercritical shocks over the same range of latitudes.

The latitudinal dependence of> 40 keV ion and electron fluxes observed by the HISCALE (Heliospheric Instrument for Spectra, Composition and Anisotropy at Low Energies) [Simnett, 1994] is consistent with measures of shock strength, such as Mach number or shock velocity. There was a rapid increase in maximum flux as Ulysses left the ecliptic plane until 20° S latitude, after which decreases in both ion and electron flux maxima were observed. As figure 4 indicates, the strongest forward and reverse shocks are observed in this range.

Acknowledgements The research described in this publication was carried out by the Jet Propulsion Laboratory, California Institute of Technology, under a contract with the National Aeronautics and Space Administration. Support for the magnetic field investigation at Imperial College is provided by the U.K. Particle Physics and Astronomy Research Council.

References

Abraham-Shrauner, B., and S.H. Yun, Interplanetary shocks seen by Ames plasma probe on Pioneer 6 and 7, *J. Geophys. Res*, 81, 2097, 1976.

Balogh, A., T.J. Beek, R.J. Forsyth, P.C. Hedgecock, R.J. Marquedant, E.J. Smith, D.J. Southwood and B.T. Tsurutani, The magnetic field investigation on the Ulysses mission: instrumentation and preliminary scientific results, *Astron. Astrophys. Suppl.*, 92, 221, 1992.

Balogh, A., J.A. Gonzalez-Esparza, R.J. Forsyth, M.E. Burton, B.E. Goldstein E.J. Smith and S.J. Bame, Interplanetary shock waves: Ulysses observations in and out of the ecliptic plane. *Space Science Reviews, 72, 171,1995.*

Bame, S. J., D.J. McComas, B. I.. Barraclough, J.L. Phillips, K.J. Sofaly, J.C. Chavez, B.E. Goldstein, The Ulysses solar wind plasma experiment, *Astron. Astrophys. Suppl.*, *92, 237,* 1992.

Burton, M. E., E.J. Smith, B.E. Goldstein, A. Balogh, R.J. Forsyth, and S.J. Bame, Ulysses: Interplanetary shocks between 1 and 4 AU, *Geophys. Res Letters, 19, 1287,1992.*

Colburn, D.S. and C. P. Sonett, Discontinuities in the solar wind, *Space Sci. Rev., 5, 439, 1966.*

Gonzalez-Esparza, J. A., A. Balogh, R.J. Forsyth, M. Neugebauer, E.J. Smith and J.L. Phillips, Interplanetary shock waves and large-scale structures: Ulysses observations in and out of the ecliptic plane, submitted to *J. Geophys. Res.,* 1996.

Gosling, J. T., S.J. Bame, D.J. McComas, J.L. Phillips, V.J. Pizzo, B.E. Goldstein, and M. Neugebauer, Latitudinal variation of solar wind corotating stream interaction regions: Ulysses, *Geophys. Res. Lett., 20,2789-2792, 1993.*

Gosling, J. T., W.C. Feldman, D.J. McComas, J. I.. Phillips, V.J. Pizzo and R.J. Forsyth, Ulysses observations of opposed tilts of solar wind corotating interaction regions in the northern and southern solar hemispheres. *Geophys. Res Left.,* 22, 3333,1995.

Kennel, C. F., Critical math numbers in classical magnetohydrodynamics, *J. Geophys. Res.*, 92, 13427, 1987.

Phillips, J. L., A. Balogh, S.J. Bame, B.E. Goldstein, J.T. Gosling, J.T. Hoeksema, D.J. McComas, M. Neugebauer, Ulysses at 50° south: constant immersion in the high-speed solar wind, Geophys. *Res Lett.*, 21,1105,1994.

Pizzo, V.J. A three-dimensional model of corotating streams in the solar wind. 3 Magnetohydrodynamic streams, *J. Geophys. Res.*, 87, 4374, 1982.

Pizzo, V.J. The evolution of corotating stream fronts near the ecliptic plane in the inner solar system 2. Three-dimensional tilted-dipole fronts, *J. Geophys. Res.*, 96, 5405,1991.

Pizzo, V. J., Global, quasi-steady dynamics of the distant solar wind. 1. Origin of north-south flows in the outer heliosphere, *J. Geophys. Res.* , 99, 4173, 1994.

Sanderson, T. R., R.G. Marsden K.-P. Wenzel, A. Balogh, R.J. Forsyth and B.E. Goldstein, Ulysses high-latitude observations of ions accelerated by co-rotating interaction regions, *Geophys. Res Lett.*, 21, 1113,1994

Simnett, G.M. K. Sayle, E.C. Roelof and S.J. Tappin, Corotating particle enhancements out of the ecliptic plane, *Geophys. Res Lett.*, 21, 1561,1994. .

Siscoe, G.L. Three-dimensional aspects of interplanetary shock waves, *J. Geophys. Res.* , 81, 6235, 1976.

Smith, E.J. Interplanetary Shock Phenomena Beyond 1 Au, in Collisionless Shocks in the Heliosphere: Reviews of Current Research, American Geophysical Union, Washington, D.C. Monograph, B.T. Tsurutani and R.G. Stone, editors, pp. 69-83, 1985.

Smith, E.J. and M.E. Burton, Shock analysis: Three useful new relationships, *J. Geophys. Res.*, 93, 2730, 1988.

Smith, E. J., M. Neugebauer, A. Balogh, S.J. Bame, G. Erdos, R.J. Forsyth, B.E. Goldstein, J.L. Phillips and B.T. Tsurutani, Disappearance of the heliospheric sector structure at Ulysses, *Geophys. Res Lett.*, *20, 2327,1993.*

Smith, E. J., M. Neugebauer, A. Balogh, S.J. Bame, R.P. Lepping and B.T. Tsurutani, Ulysses observations of latitude gradients in the heliospheric magnetic field: radial component and variances, *Space Sci. Rev., 72, 165, 1995.*

Solar Geophysical Data, Preliminary Report and Forecast, NOAA-USAF Space Environment Services Center, Boulder, CO, SESC PFR 853-956, 1992-3.

Sonnerup, B.O. and L.J. Cahill Jr., Magnetopause Structure and Attitude from Explorer 12 Observations, *J. Geophys. Res., 72, 171, 1967.*

Volkmer, P.M. and F.M. Neubauer, Statistical properties of fast magnetoacoustic shock waves in the solar wind between 0.3 and 1 AU: Helios 1,2, *Ann. Geophys,* 3, *1,* 1985.

Figure Captions

figure 1. Hourly averages Ulysses observations of magnetic field magnitude and solar wind velocity from post-Jupiter through the end of 1993. The radial distance and heliographic latitude are shown at the top of the |B| panels. Forward shocks are indicated by an up-arrow and reverse shocks by a down-arrow. This time period is divided into four intervals , A,B,C and D for varying solar wind conditions as described in the text.

figure 2 Frequency (#/day) of forward (squares), reverse (triangles), and total number of shocks (circles) observed at Ulysses throughout the interval of this study.

figure 3. θ_{BN}, beta and Mach number, as a function of heliographic latitude. The bin size is increased with increasing heliographic latitude to acquire sufficient data to calculate bin averages. The average is plotted in the center of the bin.

figure 4. Various parameters indicating shock strength plotted as a function of heliographic latitude. The top panel is the ratio of the upstream to downstream field magnitude, the middle panel is the shock velocity and the bottom panel is the ratio of math number to first critical math number.

figure 5. Angle between the shock normal the magnetic dipole axis normalized for solid angle effect (described in the text) and plotted separately for forward and reverse corotating shocks.

figure 6. Shock normal directions fo, corotating shocks plotted in the r, δ plane shown separately for forward and reverse shocks.

figure 7. Configuration of solar corona (top panel) and corresponding neutral line contour for Barrington rotation 1860 and typical of the interval of the study.

figure 8. Ion density and ion beta computed over five degree latitude intervals.

figure 9. Comparison of actual θ_{BN} for corotating shocks (bottom panel) with a "synthetic" value (top panel) calculated by assuming the shock normal is perpendicular to the Parker spiral.

figure 10. Peak total pressure (magnetic field plus plasma) at the interfaces between the slow and fast solar wind.

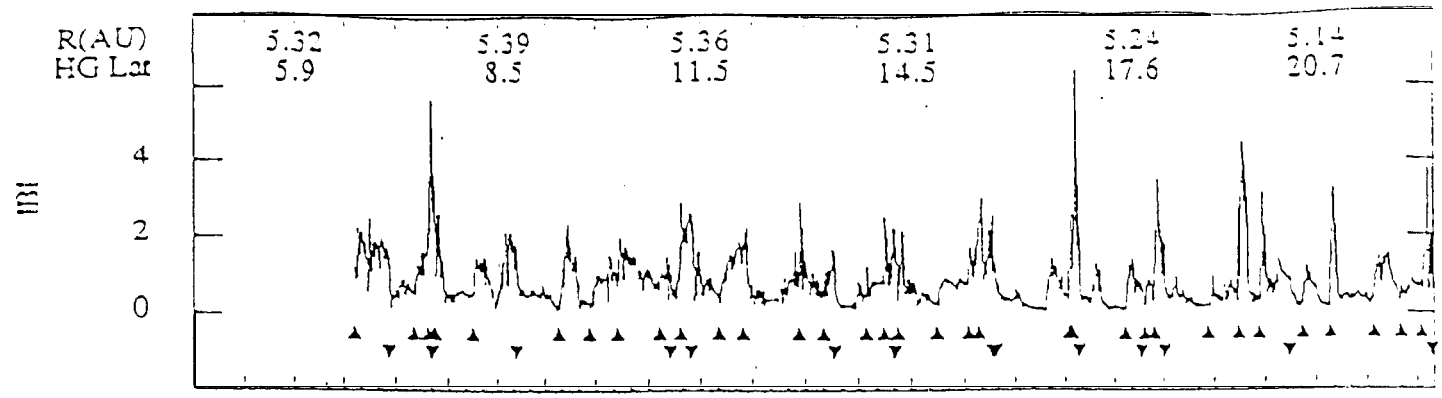
R(AU)
HG Lat
5.32
5.9
5.39
8.5
5.36
11.5
5.31
14.5
5.24
17.6
5.14
20.7
IBI
4
2
0

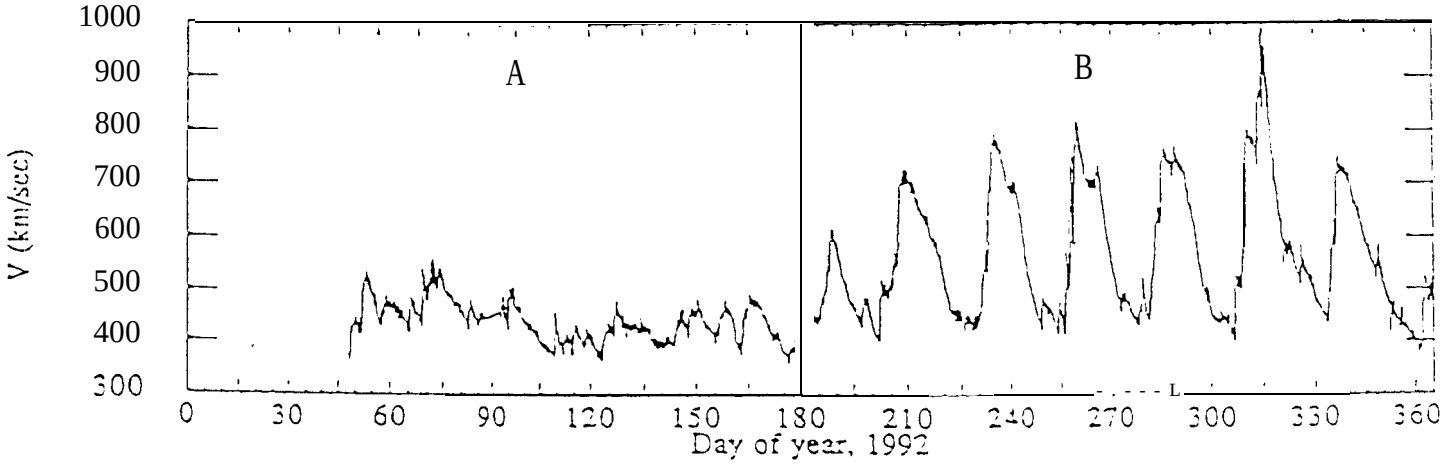
V (km/sec)
1000
900
800
700
600
500
400
300
A
B
0
30
60
90
120
150
180
210
240
270
300
330
360
Day of year, 1992

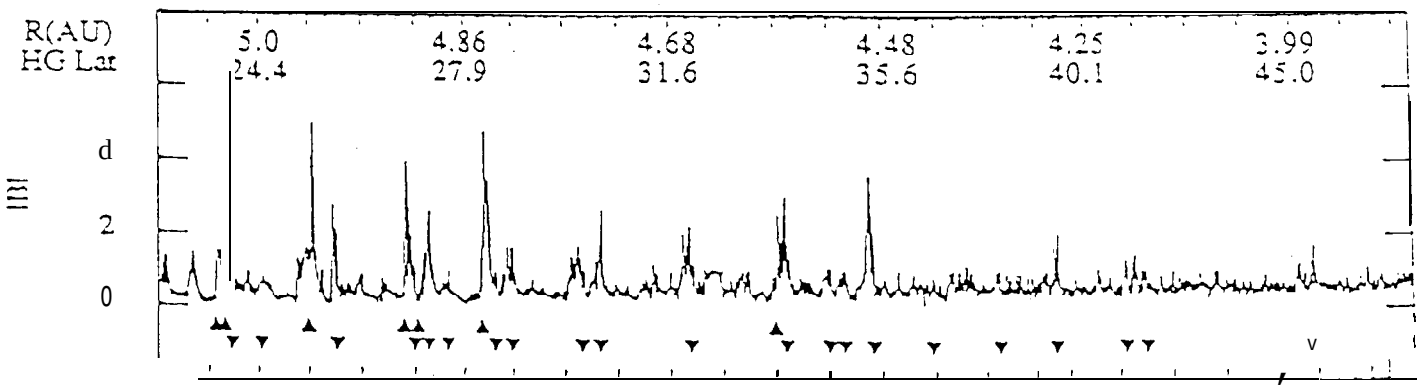
R(AU)
HG Lat
5.0
24.4
4.86
27.9
4.68
31.6
4.48
35.6
4.25
40.1
3.99
45.0
IBI
d
2
0

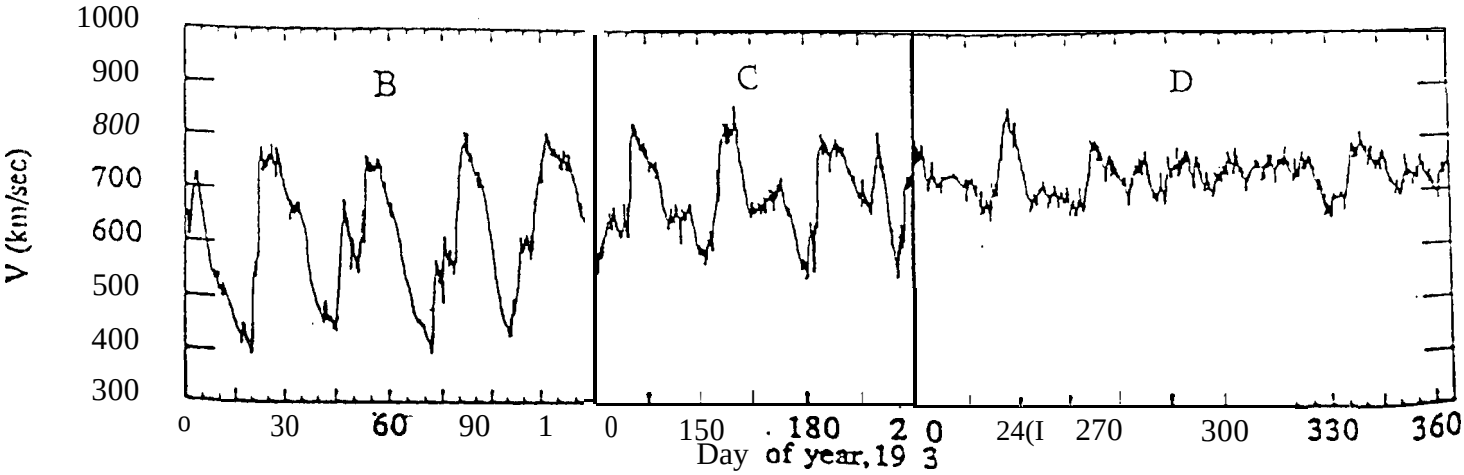
V (km/sec)
1000
900
800
700
600
500
400
300
B
C
D
0
30
60
90
150
180
210
240
270
300
330
360
Day of year, 1993

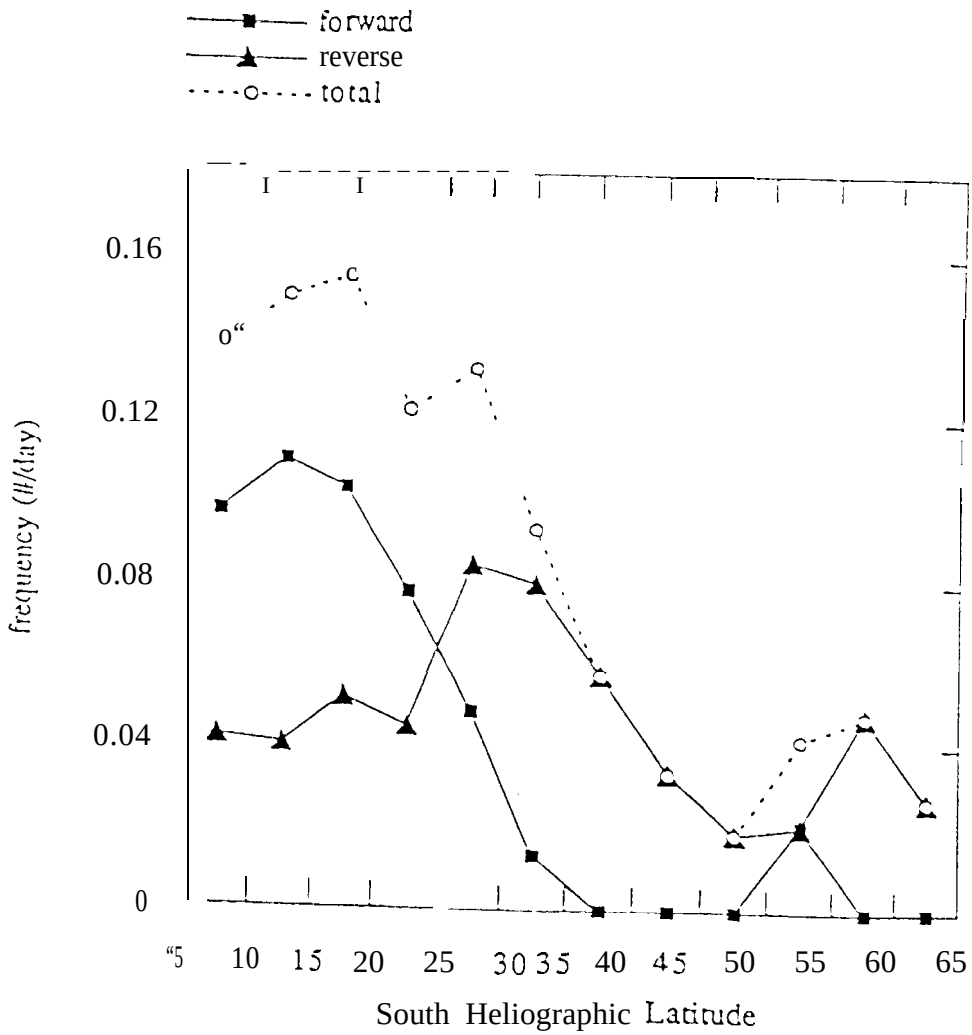
forward
reverse
total
0.16
0.12
0.08
0.04
0
frequency (#/day)
10
15
20
25
30
35
40
45
50
55
60
65
South Heliographic Latitude

figure 2

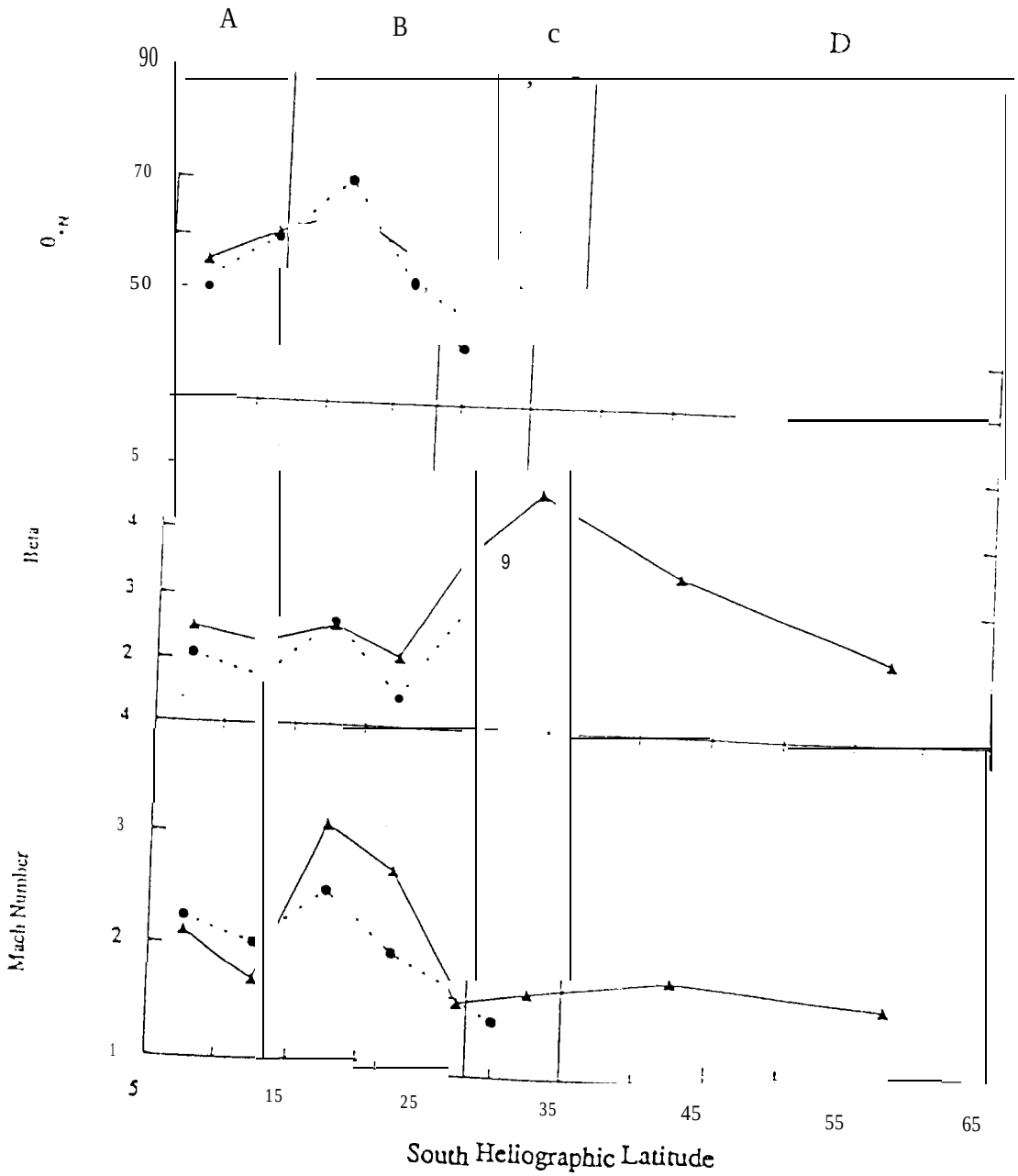
A
B
c
D
90
70
50
5
4
3
2
4
3
2
1
5
9
15
25
35
45
55
65
Beta
Mach Number
South Heliographic Latitude

figure 3

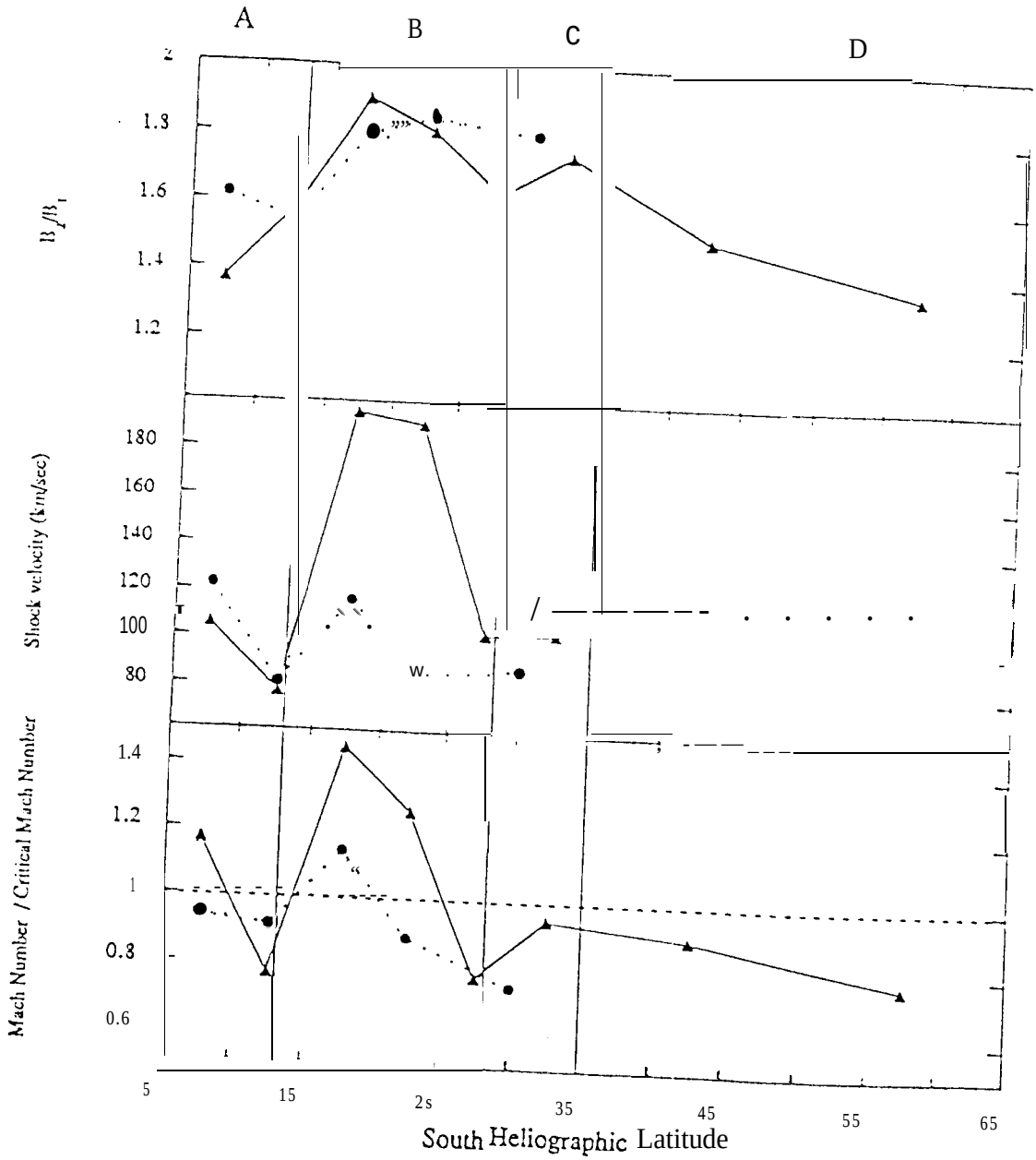
A
B
C
D
1.8
1.6
1.4
1.2
180
160
140
120
100
80
1.4
1.2
1
0.8
0.6
5
15
25
35
45
55
65
South Heliographic Latitude
Shock velocity (km/sec)
Mach Number / Critical Mach Number

figure 4

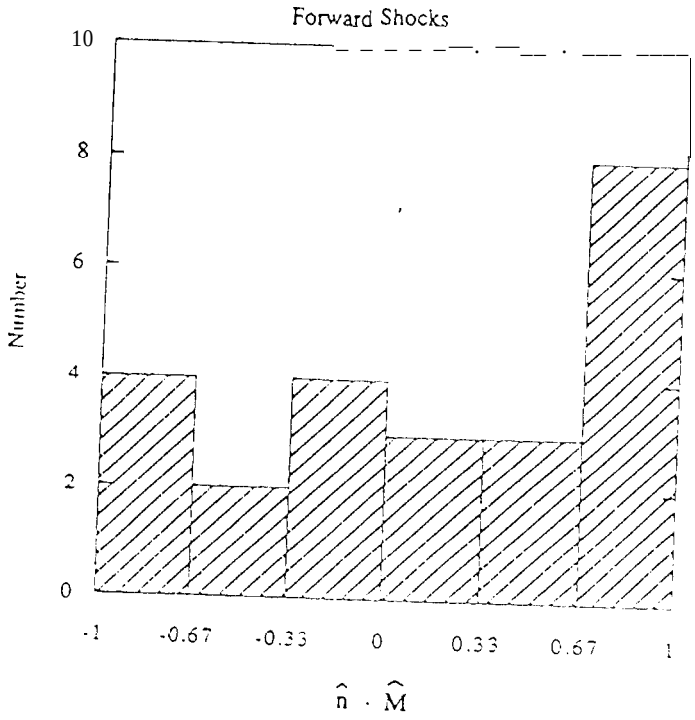
Forward Shocks
Number
10
8
6
4
2
0
-1
-0.67
-0.33
0
0.33
0.67
1
n̂ · M̂

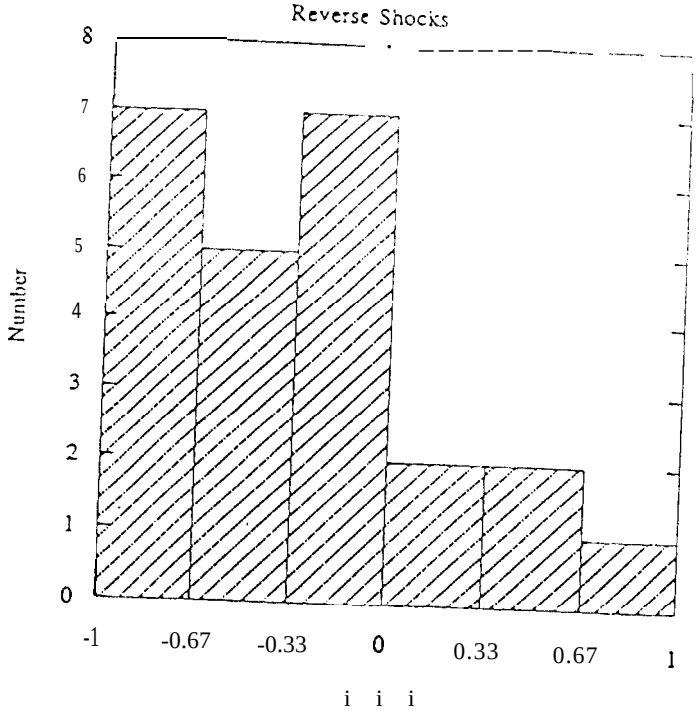
Reverse Shocks
Number
8
7
6
5
4
3
2
1
0
-1
-0.67
-0.33
0
0.33
0.67
1

figure 5

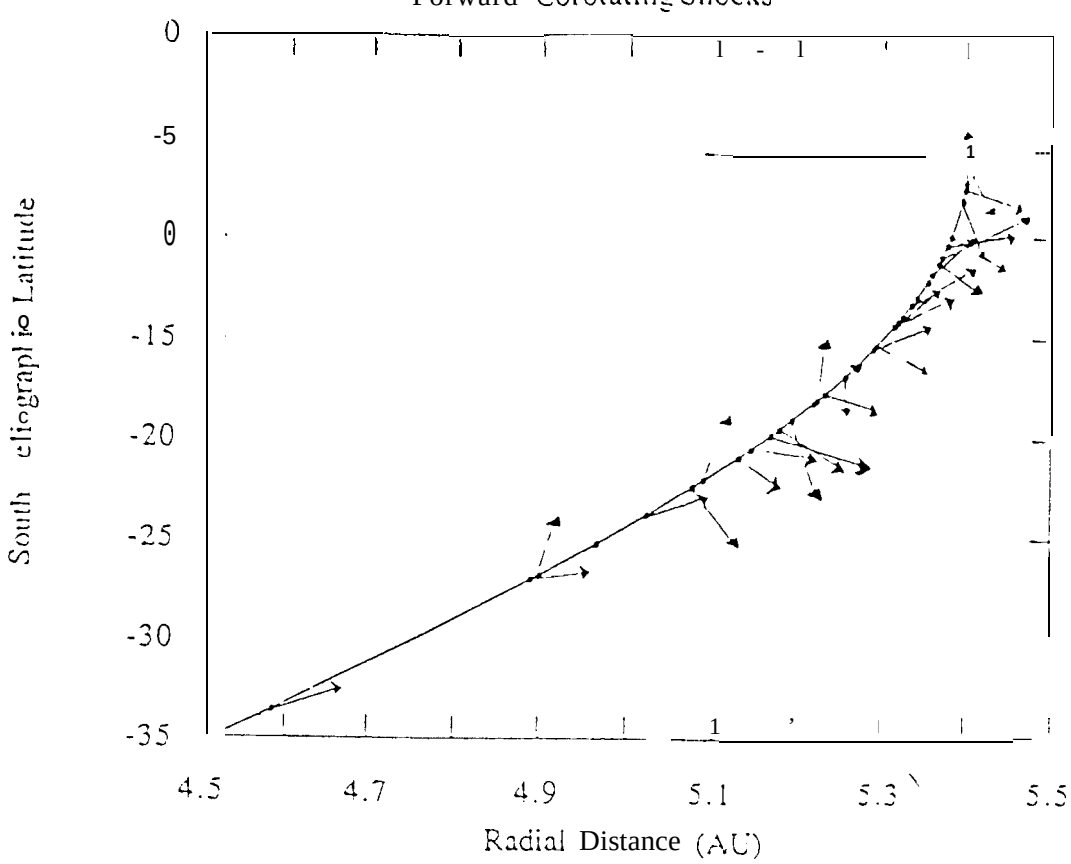
Forward Corotating Shocks
0
-5
0
-15
-20
-25
-30
-35
South eliegrapl io Latitude
4.5
4.7
4.9
5.1
5.3
5.5
Radial Distance (AU)

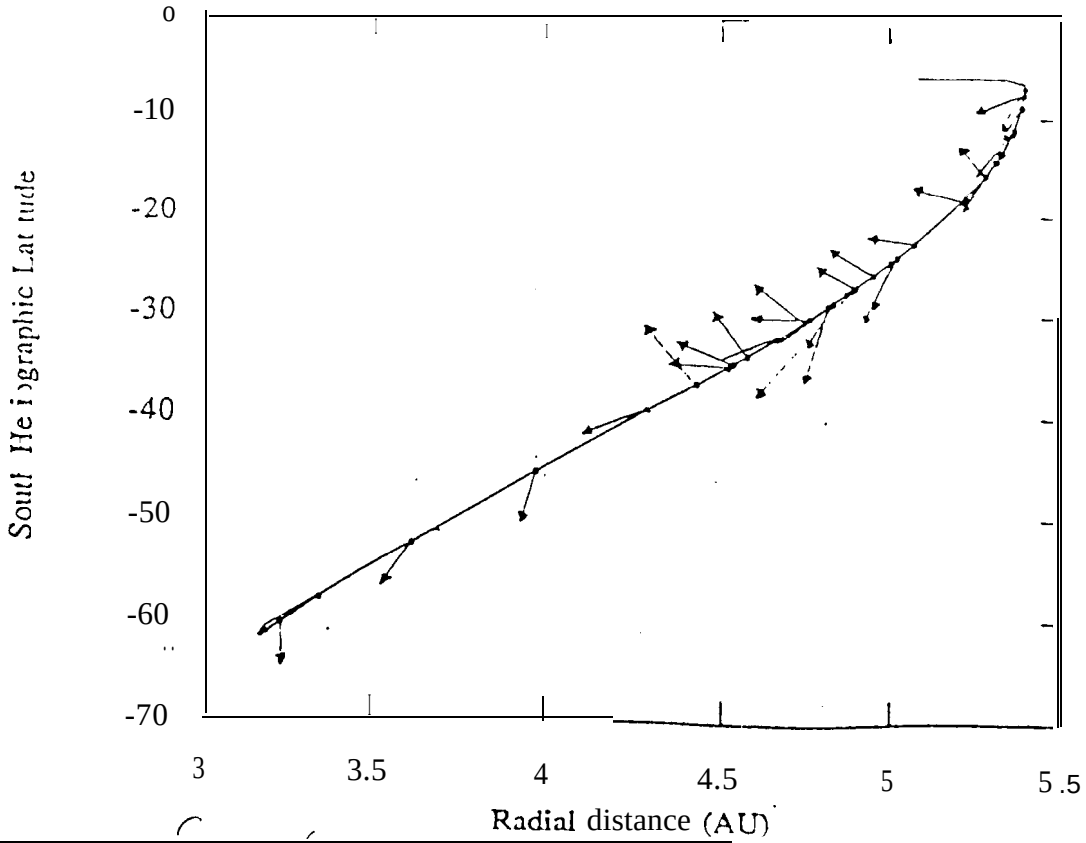
0
-10
-20
-30
-40
-50
-60
-70
Soutl He i ographic Lat tude
3
3.5
4
4.5
5
5.5
Radial distance (AU)

N

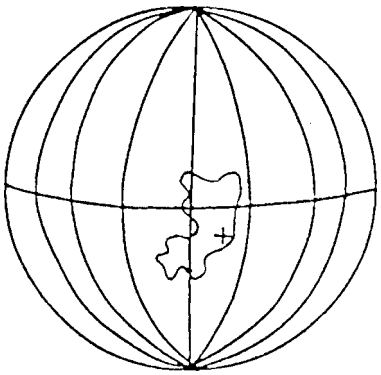

1636 UT
9/28/92

SOLAR MAGNETIC FIELD SYNOPTIC CHART

SOURCE SURFACE FIELD
CARRINGTON ROTATION NUMBER 1860
(6 September to 3 October 1992)

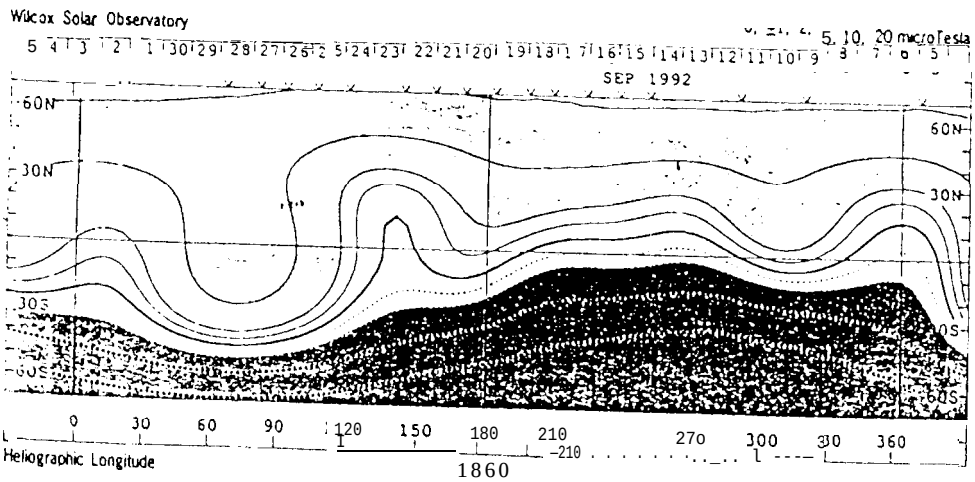

1860

figure 7

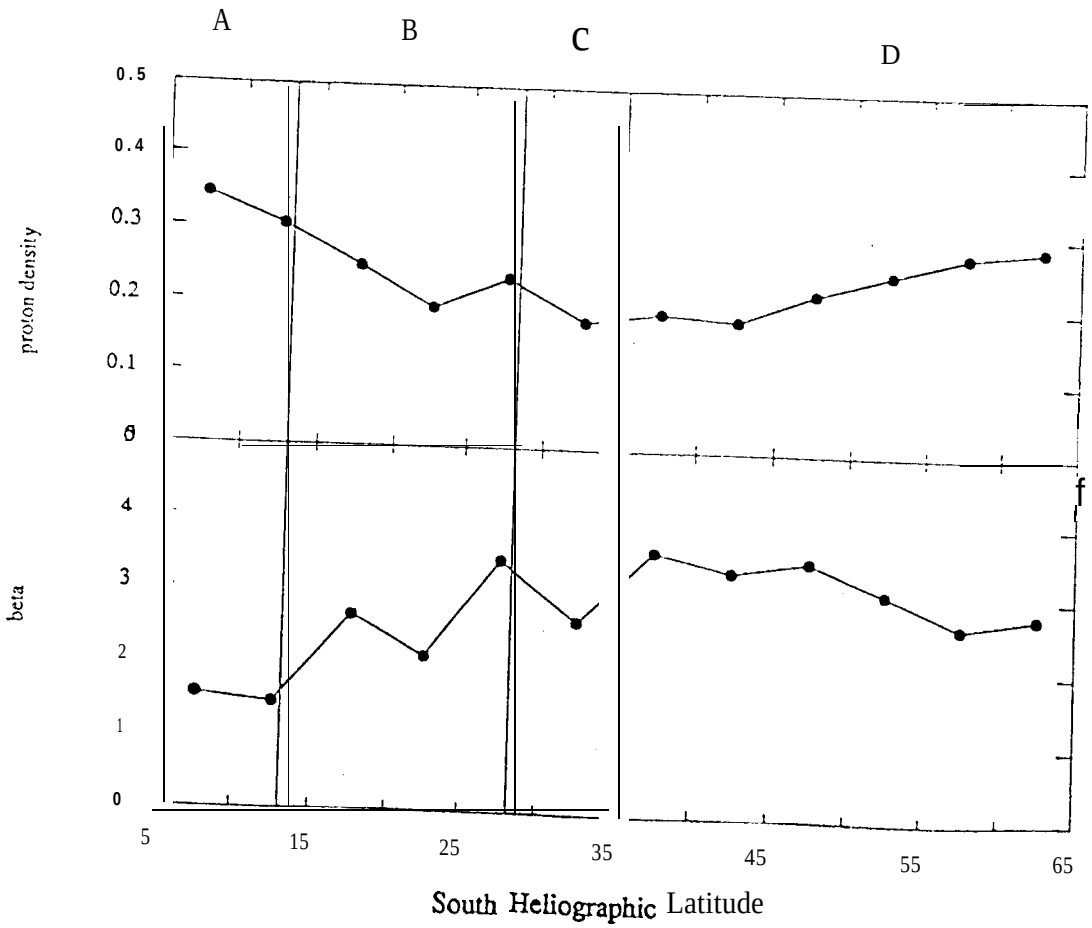
A
B
C
D
0.5
0.4
0.3
0.2
0.1
0
4
3
2
1
0
proton density
beta
5
15
25
35
45
55
65
South Heliographic Latitude

figure 8

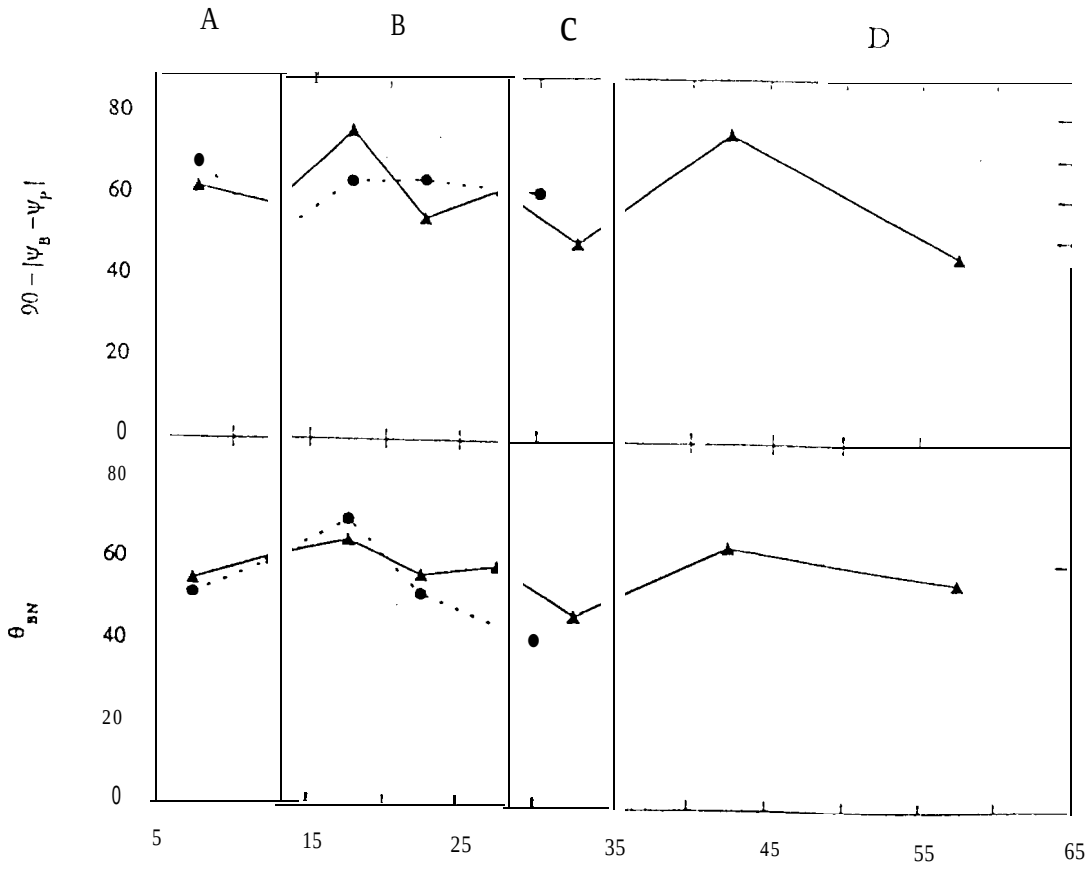
A
B
C
D
80
60
40
20
0
$90-|\psi_B-\psi_P|$
80
60
40
20
0
θ_{BN}
5
15
25
35
45
55
65
South Heliographic Latitude

figure 9

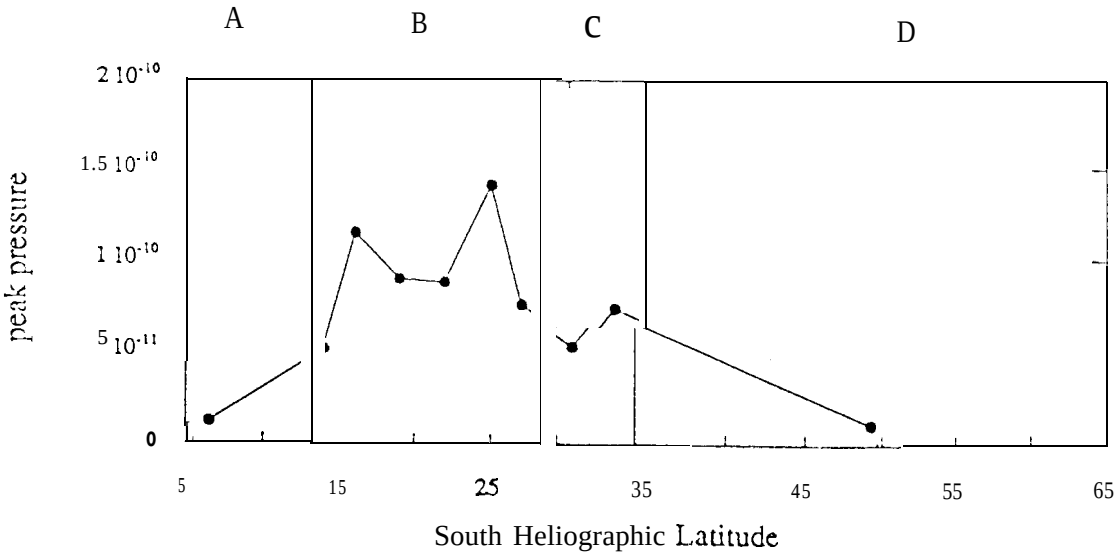
A
B
C
D
2 10-10
1.5 10-10
1 10-10
5 10-11
0
peak pressure
5
15
25
35
45
55
65
South Heliographic Latitude

figure 10